https://doi.org/10.5194/egusphere-2023-1397
Preprint. Discussion started: 28 July 2023

The staggered retreat of grounded ice in Ross Sea, Antarctica since the LGM

Matthew A. Danielson[1], Philip J. Bart[1]

[1]Department of Geology and Geophysics, Louisiana State University, Howe-Russell Geoscience Complex E235, Baton Rouge, LA 70803, USA

Correspondence to: Matthew A. Danielson (mdani38@lsu.edu)

Abstract.

The post-LGM retreat of the West Antarctic Ice Sheet (WAIS) in Ross Sea was greater than for any other Antarctic sector. Here we combined the available chronology of retreat with new mapping of seismically-resolvable grounding zone wedges (GZWs). Mapping GZWs is important because they record the locations and durations of former stillstands in the extent of grounded ice for individual ice streams during the overall retreat. Our analysis shows that the longest stillstands occurred early in the deglacial and had millennial durations. Stillstands ended abruptly with retreat distances measured in the tens to hundreds of kilometers creating deep embayments in the extent of grounded ice across Ross Sea. The location of embayments shifted through time. The available chronological data shows that cessation of WAIS stillstands was highly asynchronous across at least five thousand radiocarbon years. There was a general shift to shorter stillstands as the deglacial progressed. Asynchronous collapse of individual catchments over the course of the post-LGM suggests that the Ross Sea sector would have contributed to multiple episodes of relatively-small amplitude, sea-level rise. The high sinuosity of the modern ground zone in Ross Sea suggests that this style of retreat persists.

https://doi.org/10.5194/egusphere-2023-1397
Preprint. Discussion started: 28 July 2023

1 Introduction

By the peak of the LGM, grounded ice had advanced to the outer-most continental shelf in western Ross Sea (wRS) Antarctica and to the continental shelf edge in eastern Ross Sea (eRS) (Anderson et al., 2014). In other words, the extent of grounded and floating ice was nearly as expansive as it could possibly have been. At that time, six fast flowing ice streams deeply eroded broad and foredeepened troughs across the continental shelf. Eroded sediment was transported in basal ice and/or subglacially (Alley et al., 1989; Powell et al., 1996; Alley et al., 2007; Christoffersen et al., 2010; Prothro et al., 2018). The sediment was ultimately deposited either on the outer continental shelf (OCS) or upper slope depocenters (Shipp et al., 1999). In the wRS, foredeepened troughs Drygalski Trough (DT), JOIDES Basin (JB), and Pennell Trough (PT) extend to the continental shelf edge and were eroded during several successive glacial maxima. The outer part of these troughs were then partly back filled with large-scale grounding zone wedges (GZWs) during and/or after the LGM. In the eRS troughs, where ice had reached the continental shelf edge, large trough-mouth fans were deposited on the upper slope (Mosola and Anderson, 2006). The ice sheet retreated during the post-LGM but paused within the outer reaches of the Glomar Challenger Basin (GCB), Whales Deep Basin (WDB) and Little America Basin (LAB), sufficiently long to deposit large GZWs (i.e., several tens of meters thick and tens of kilometers long) (Mosola and Anderson, 2006; Bart and Owolana, 2012) . The GZW sediment volumes partly reflect durations of grounding-line stillstands for individual ice streams (Bart and Cone, 2012; Bart and Owolana, 2012; Bart et al., 2017). Several previous studies have focused on the changing extent of grounded and floating ice and timing of post-LGM retreat (Conway et al., 1999; Domack et al., 1999; Mosola and Anderson, 2006). Anderson et al. (2014) conducted the last Ross-Sea wide synthesis of seismic stratigraphy and radiocarbon dates. More recently, Halberstadt et al. (2016) conducted a detailed evaluation of legacy multibeam data and identified GZWs and mega-scale glacial lineations associated with the LGM and post-LGM GZW stillstands. These stratigraphic data provide abundant evidence as to the progression of WAIS retreat based on stratigraphic superposition. Here we build on the Halberstadt et al. (2016) study of seafloor morphology by mapping the sediment volume of the GZWs across the six basins of Ross Sea to evaluate the duration of individual grounding-zone

https://doi.org/10.5194/egusphere-2023-1397
Preprint. Discussion started: 28 July 2023

stillstands. Establishing the former durations of GZWs is important to understand the Ross Sea-wide regional scale ice-sheet retreat and thus how ice-volume changes from Antarctica contributed to global sea-level in the past. The paleo-perspective also informs our understanding of how additional contraction might proceed and contribute to future sea-level rise.

2 Methods

2.1 Regional seismic grid

Our study generated regional stratigraphic correlations of regional bounding surfaces across 22 surveys of multi- and single-channel reflection seismic data acquired from across the Ross Sea (Supplemental Table 1). The surveys include 510 seismic lines with a total coverage of ~54,000 km. The data are currently stored and maintained at the Antarctic seismic data library system (SDLS) at the Italian National Institute of Oceanography and Applied Geophysics (OGS) and have been used in previous studies such as Perez et al. (2021). Our mapping focused on GZWs interpreted to be of LGM and post-LGM ages complementing the analyses of seafloor morphology by Halberstadt et al. (2016). The seismic surveys were interpreted in the Petrel software (Figure 1). The digital data used in this study have been processed prior to being archived at the SDLS. Individual seismic lines were imported as segy files into the software using separate files containing navigation data.

https://doi.org/10.5194/egusphere-2023-1397
Preprint. Discussion started: 28 July 2023

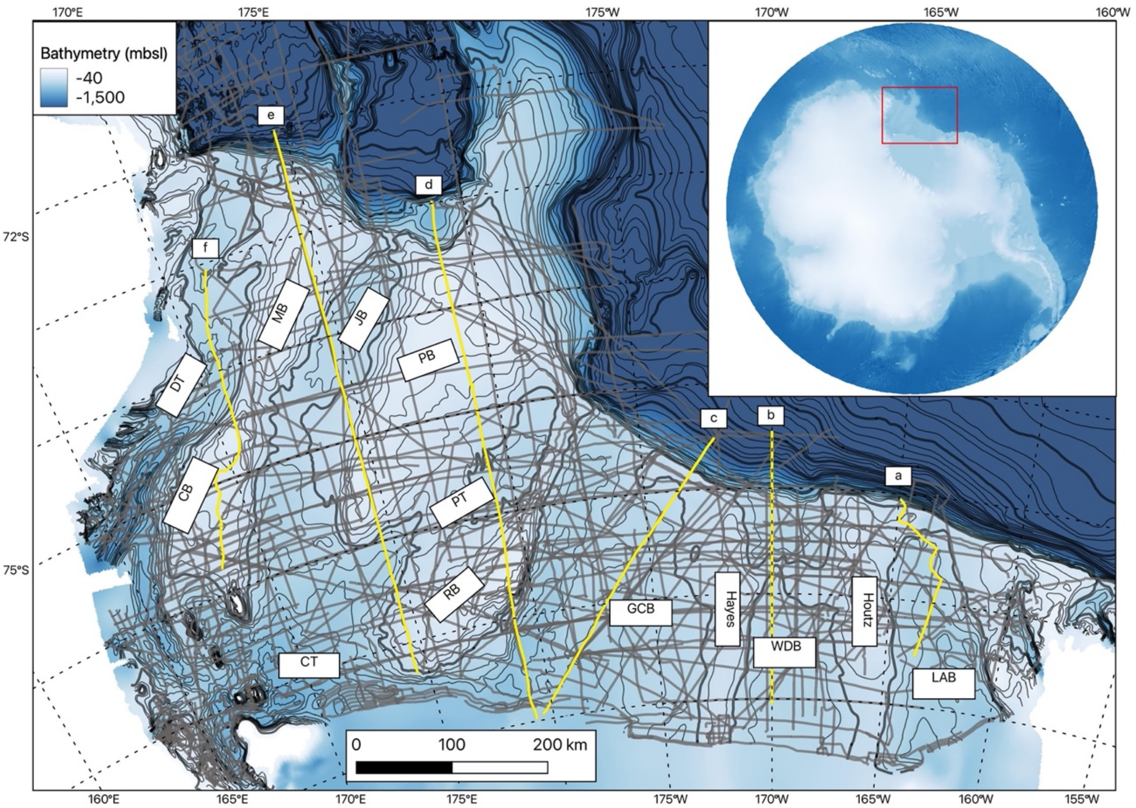

Figure 1: Map of Ross Sea showing seismic coverage. Bathymetry is from Davey and Nitsche (2013). Inset map of Antarctica using the International Bathymetric Chart of the Southern Ocean ice surface and bathymetry grid showing the location of Ross Sea in the red box. LAB = Little America Basin, WDB = Whales Deep Basin, GCB = Glomar Challenger Basin, PT = Pennell Trough, CT = Central Trough, JB = JOIDES Basin, DT = Drygalski Trough. Letters indicate the positions of composite seismic lines through each trough shown in Supplemental Figure 2.

2.2 LGM and post-LGM seismic interpretation and isopach mapping

We focused on the seismically-resolvable LGM and post-LGM GZWs throughout Ross Sea that have been identified in previous seismic studies (Shipp et al., 1999; Mosola and Anderson, 2006; Bart and De Santis, 2012; Bart and Owolana, 2012; Bart et al., 2017). This includes GZWs identified in legacy multibeam data (Halberstadt et al., 2016). The seafloor reflection and the unconformities bounding the top and base of the GZWs were mapped using regional seismic stratigraphy and comparison to previous studies. The horizons were mapped for each 2D line to delineate the seafloor reflection and the unconformities bounding the major GZWs in each trough on the continental shelf. Additional single channel paper seismic

https://doi.org/10.5194/egusphere-2023-1397
Preprint. Discussion started: 28 July 2023

lines from four surveys (NBP9307, NBP9401, NBP9501 and NBP9902) were used to supplement the interpretation of major GZW features. These interpretations were completed on paper and then imported into Petrel using navigation files as a set of points in two-way travel time.

Two-way-travel time maps were made using convergent interpolation in the Petrel software with a cell size of 50 meters where the computer-interpreted horizons were the primary input, and the paper-interpreted data were secondary input. Time-structure maps were made by subtracting the map of the GZW base from the seafloor map. Refraction sonobuoy measurements in the Ross Sea provide a regional record of sediment velocities (Cochrane et al., 1992; Cochrane et al., 1995). The points of the sonobuoy measurements taken from four expeditions were plotted in Petrel (Supplemental Table 2). Interpolation between the sonobuoy locations was done to create depth and interval velocity maps. All the analyzed GZW deposits were in shallow layers of sediment (upper 250 millisecond) and thus only the uppermost interval velocity map was used. This section has velocities that vary from 1700 to 2200 meter/second across the region (Supplemental Figure 1). The interval velocity map was then used as an input to build a velocity model in Petrel. Time-structure maps were then depth-converted using the velocity model to create isopach maps for each GZW.

2.3 Volume and duration calculation

The isopach maps were used to calculate sediment volumes for the GZWs in the QGIS software. The sediment volumes were then used to estimate stillstand duration. The paleo-sediment flux for each of the paleo ice streams in Ross Sea (Equation 1) is defined as Q_s. The paleo-sediment flux of an ice stream is the produce of the paleo-drainage area (A) and average sediment yield (S). Our estimates use a simple assumption concerning the average erosion rate and paleo-drainage area. The sediment yield of 0.7 ±0.21 mm yr^{-1} derived by Bart and Tulaczyk (2020) for the WDB drainage area was applied to the adjacent catchments to infer a paleo-flux for each trough. The 0.7 ±0.21 mm yr^{-1} erosion rate was derived for the WDB middle shelf GZW which was determined to have been deposited during a stillstand whose onset and cessation dates are constrained by radiocarbon dates (Bart et al., 2018).

$$Q_s = AS \tag{1}$$

Paleo-drainage areas were estimated for each of the paleo-troughs of Ross Sea using the drainage area of the present-day WAIS ice-streams and East Antarctic outlet glaciers and projecting their extents into each of the troughs on the OCS (Figure 2). The

https://doi.org/10.5194/egusphere-2023-1397
Preprint. Discussion started: 28 July 2023

approach assumes single-ice stream capture for WDB and LAB. The GCB received drainage from the combination of Kamb, Whillans and Mercer ice streams based on the sub-ice shelf topography shown in the ROSETTA project in addition to other East Antarctic glaciers (Licht et al., 2005; Tinto et al., 2019). The JB and PT shared capture from Byrd and other smaller East Antarctic catchments while the DT primarily received ice flow from the David glacier during the LGM (Licht and Palmer, 2013; Licht et al., 2014). Grounding duration at each location was calculated using the method following Bart and Tulaczyk (2020) where ΔT is the grounding duration, V is the total volume of GZW sediment and Q_s is the paleo-sediment flux (Equation 2).

$$\Delta T = \frac{V}{Q_s} \quad (2)$$

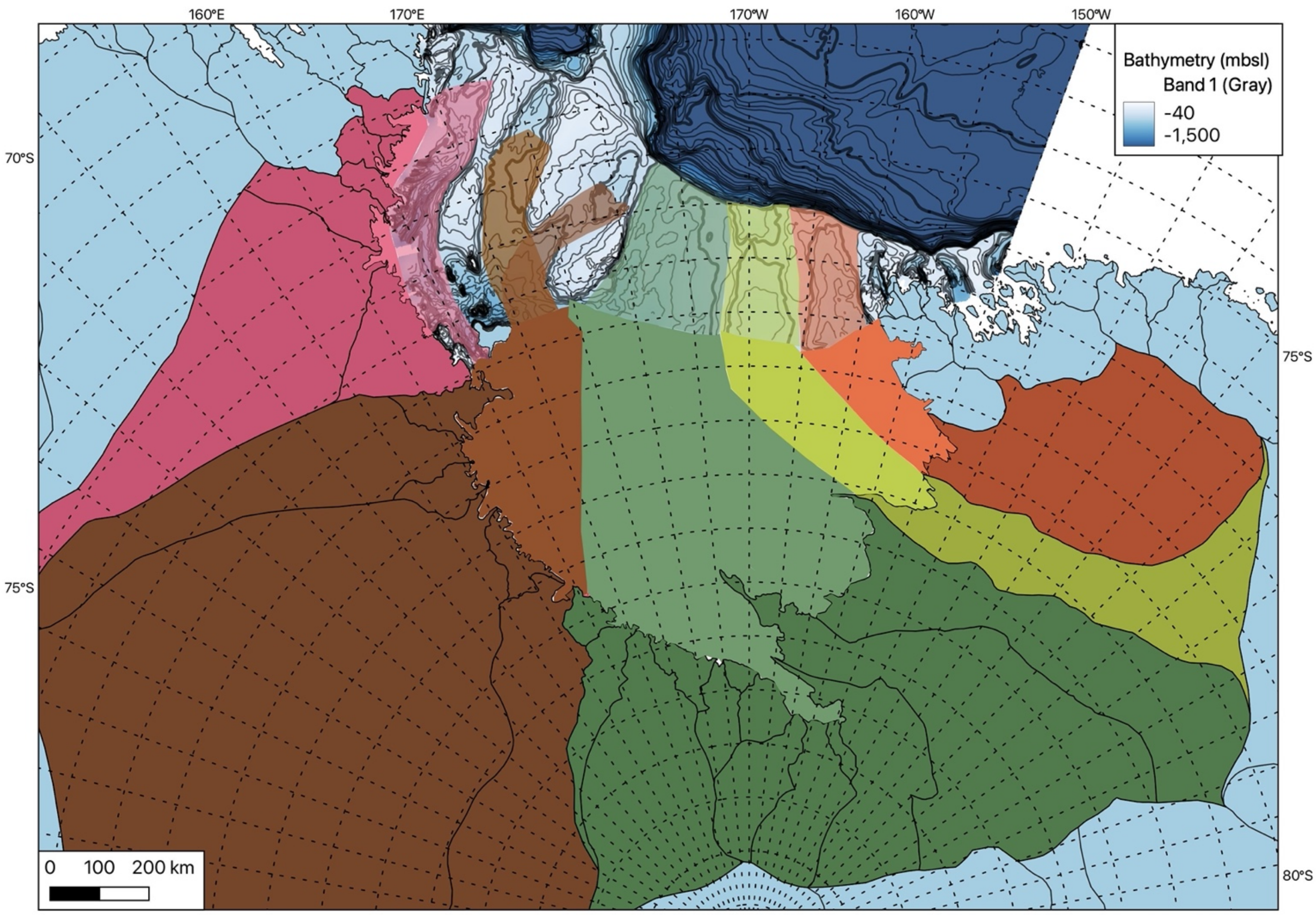

Figure 2: Estimated paleo-drainage catchments for each of the major troughs across the Ross Sea during the LGM. The darker shades correspond with the present-day drainage areas while the lighter shades correspond with the projected paleo-drainage into

https://doi.org/10.5194/egusphere-2023-1397
Preprint. Discussion started: 28 July 2023

the troughs when the ice sheet extent was expanded. Yellow = LAB, Orange = WDB, Green = GCB, Brown = Pennell and JOIDES, Pink = Drygalski Trough, JOIDES and Pennell Trough capture drainage from East Antarctic glaciers. GCB drained a combination of WAIS paleo-ice streams and East Antarctica outlet glacier flow. LAB and WDB received sediment from individual WAIS paleo-ice streams.

3 Results

3.1 Seismic-resolvable GZWs in Ross Sea

Stratigraphic correlations on the regional seismic transects yielded two-way travel time maps for the Ross Sea OCS and middle continental shelf (MCS). The inner continental shelf is covered by the Ross Ice Shelf and hence cannot be investigated. Mapped horizons bound GZWs from the base of the LGM unconformity to the seafloor (Figure 3). Seventeen GZWs were identified and mapped within the Ross Sea trough basins (Supplemental Table 3). All these GZWs have seafloor exposures. Fourteen of these GZWs (Figure 4 a-h, k-m, o-q and Table 1) have been identified from previous studies (e.g., Anderson et al., 2013; Halberstadt et al., 2016). Three new GZWs were mapped from the regional seismic data in the inner reaches of the MCS sectors of JB, PT and GCB (Figure 4 i-j, n; and Table 1). The WDB and PT have two GZWs at the shelf edge and MCS. JB has two GZWs at the MCS and in the inner reaches of the trough. The GCB, which has the largest drainage area of all the paleo ice streams, has five GZWs with one at the shelf-edge, one on the middle-shelf and three in the inner reaches of the trough (Table 2).

In eRS, the shelf edge and OCS GZWs define part of the banks. In eRS, the GZWs are trough-confined except for the inner reaches of the MCS GZWs in DB that were deposited on the banks adjacent to the foredeepened section of the trough (Baroni et al., 2022). Time structure maps were generated for the top and base of each GZW and depth converted. The difference of these two surfaces gives thickness maps for the seventeen GZWs in Ross Sea (Figure 4).

3.2 Grounding durations of Ross Sea GZWs

Sediment volumes for each GZW are shown in Table 1. The outer shelf GZWs in WDB, GCB, JB and DT are the largest with sediment volumes on the order of 10^3 km^3. The inner reaches of the MCS GZWs have the smallest volumes on the order of 10^2 km^3. The drainage area for the ice streams that deposited these GZWs includes the projected paleo-ice stream drainage

https://doi.org/10.5194/egusphere-2023-1397
Preprint. Discussion started: 28 July 2023

pathways (Figure 2) up to the topset-foreset boundary of the mapped GZW. Paleo-flux values are estimated from the product of drainage area with a constant sediment yield (i.e., average erosion rate) of 0.7 ± 0.21 mm yr^{-1} derived for the WDB (Bart and Tulacyzk, 2020). Stillstand duration was then calculated from the paleo-sediment flux and GZW sediment volumes (Tables 2 and 3).

The LAB OCS GZW has the longest duration of ~3.4 kyrs while the inner reaches of the MCS GZWs have significantly shorter durations on the order of 10^1 - 10^2 years. Durations calculations include an uncertainty of ± 2 milliseconds from uncertainty in the TWTT measurement of the GZWs as well as a ± 50 m/s uncertainty from the velocity model used to convert the TWTT maps to depth.

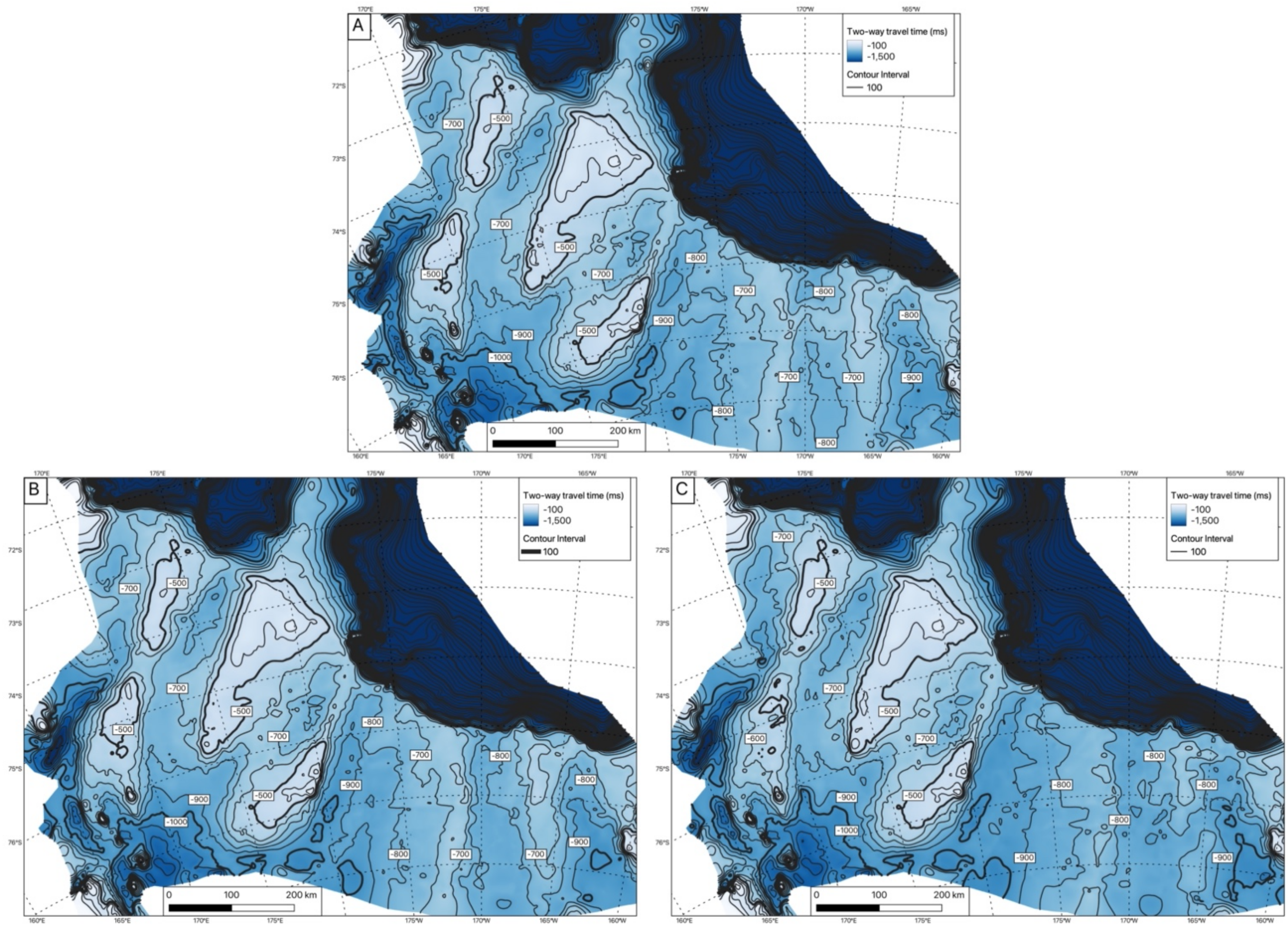

https://doi.org/10.5194/egusphere-2023-1397
Preprint. Discussion started: 28 July 2023

Figure 3: Two-way travel time contour maps of seafloor reflector (A), post-LGM unconformity (B) and the LGM unconformity (C) based on convergent interpolation of interpretations using the seismic lines shown in Figure 1. The LGM unconformity underlies the LGM age GZW complexes and is equal to the seafloor reflection in some locations. Contour interval = 100 ms.

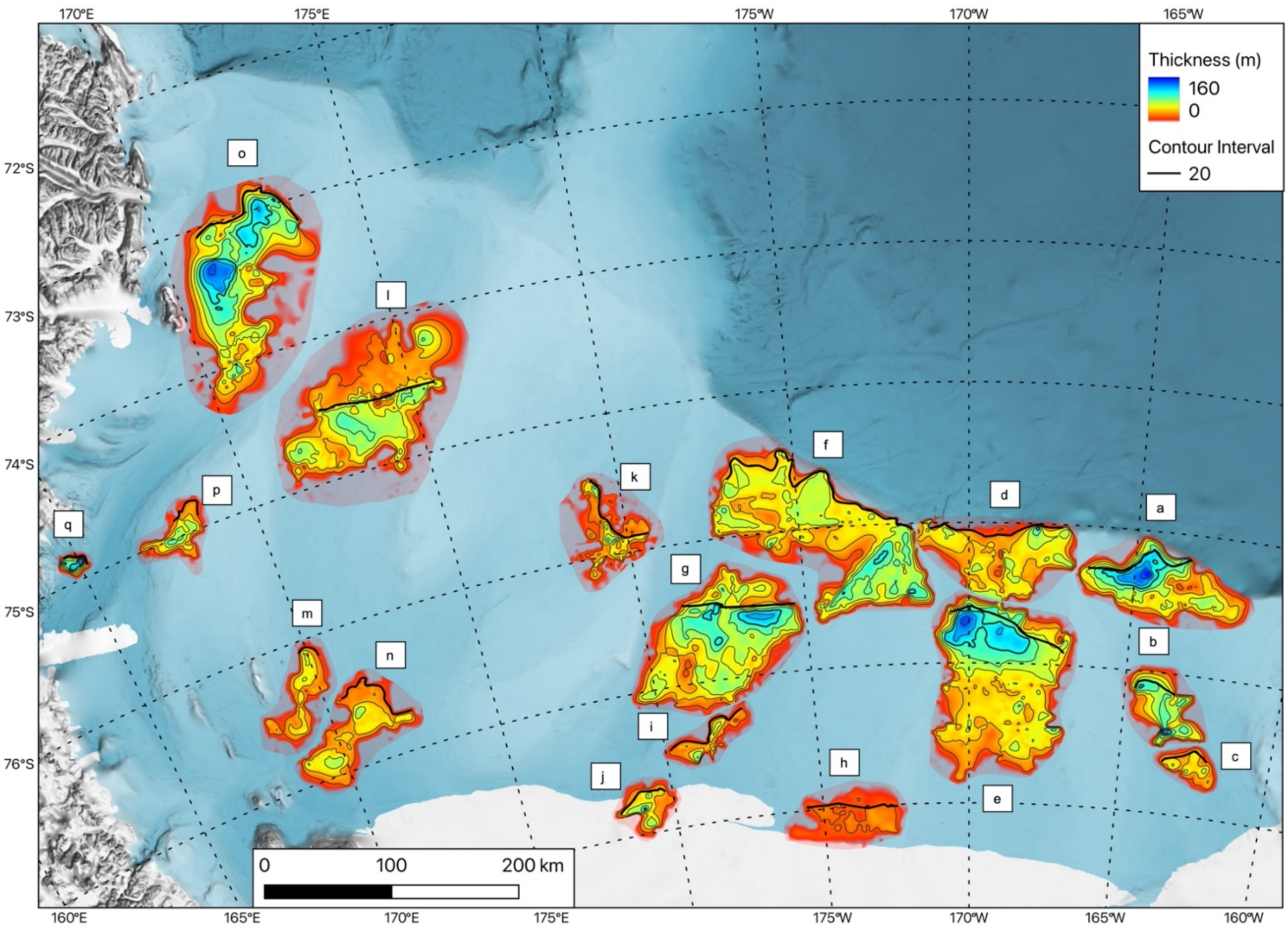

Figure 4: Thicknesses contour maps of Ross Sea GZWs. The heavy black line shows the approximate location of boundary between the GZW topset and foreset. GZWs are labeled "a" to "q" starting in the east with LAB outer shelf GZW. Letter labels of GZWs correspond with records in Table 1. Bathymetry shown in the base map is from IBSCO v2. Contour interval = 20 m

https://doi.org/10.5194/egusphere-2023-1397
Preprint. Discussion started: 28 July 2023

GZW Wedge Location	Estimated Paleo Drainage Area, *A* (km^2)	GZW Volume, *V* (km^3)	Paleo Sediment flux, *Q* (10^8 m^3 a^{-1})	Duration, ΔT (yr)
a. LAB Outer Shelf	1.25E+05	301 ± 19	0.87 ± 0.26	3445 ± 1136
b. LAB Middle Shelf	1.11E+05	120 ± 8	0.79 ± 0.23	1535 ± 506
c. LAB Middle Shelf Inner Reaches	1.05E+05	33 ± 3	0.74 ± 0.22	453 ± 149
d. WDB Outer Shelf	2.31E+05	216 ± 16	1.62 ± 0.49	1027 ± 419
e. WDB Middle Shelf	2.23E+05	534 ± 35	1.67 ± 0.47	3200 ± 700
f. GCB Outer Shelf	6.32E+05	610 ± 41	4.42 ± 1.33	1379 ± 455
g. GCB Middle Shelf West	6.17E+05	523 ± 33	4.32± 1.30	1211 ± 399
h. GCB Inner Reaches East	5.80E+05	47 ± 7	4.06 ± 1.22	116 ± 38
i. GCB Inner Reaches West	5.93E+05	33 ± 4	4.15 ± 1.24	81 ± 27
j. GCB Inner Reaches Ross Bank	5.72E+05	45 ± 4	4.00E ± 1.20	111 ± 37
k. PT Middle Shelf	1.63E+05	69 ± 8	1.14 ± 0.34	604 ± 199
l. JOIDES Middle Shelf	1.75E+05	421 ± 37	1.23 ± 0.37	3433 ± 1132
m. JOIDES Inner Reaches 1	1.48E+05	117 ± 11	1.04 ± 0.31	1128 ± 372
n. JOIDES Inner Reaches 2	1.48E+05	58 ± 6	1.04 ± 0.31	564 ± 186
o. DT Outer Shelf	3.65E+05	583 ± 21	2.56 ± 0.77	2280 ± 752
p. DT Inner Reaches 1	3.40E+05	48 ± 5	2.26 ± 0.68	204 ± 67
q. DT Inner Reaches 2	3.40E+05	20 ± 1	2.26 ± 0.68	85 ± 28

Table 1: Summary table of GZWs shown in Figure 4 with drainage area, volume, paleo sediment flux and duration with respective uncertainties.

https://doi.org/10.5194/egusphere-2023-1397
Preprint. Discussion started: 28 July 2023

	Little America	Whales Deep	Glomar Challenger	Pennell	JOIDES	Drygalski
Drainage area (km^2)	1.25E+05	2.31E+05	6.32E+05	1.63E+05	1.75E+05	3.65E+05
LGM Paleo-sediment flux (10^8 m^3 a^{-1})	0.87 ± 0.26	1.62 ± 0.49	4.42 ± 1.33	1.14 ± 0.34	1.23 ± 0.37	2.56 ± 0.77

Table 2: Drainage areas and Paleo-flux of LGM positions with respective uncertainties.

Stratigraphic superpositions	Little America	Whales Deep	Glomar Challenger	Pennell	JOIDES	Drygalski
1. OCS	301 ± 19	216 ± 16	610 ± 41			583 ± 21
2. MCS	120 ± 8	534 ± 35	523 ± 33	69 ± 8	421 ± 37	
3. IR MCS	33 ± 3		47 ± 7, 45 ± 4, 33 ± 4		117 ± 11, 58 ± 6	48 ± 5, 20 ± 1

Table 3: GZW Volumes (km^3) arranged by Ross Sea shelf position with uncertainty. OCS = outer continental shelf; MCS = middle continental shelf; IR = inner reaches.

Stratigraphic superpositions	Little America	Whales Deep	Glomar Challenger	Pennell	JOIDES	Drygalski
1. OCS	3445 ± 1136	1027 ± 419	1379 ± 455			2280 ± 752
2. MCS	1535 ± 506	3200 ± 700	1211 ± 399	604 ± 199	3433 ± 1132	
3. IR MCS	453 ± 149		116 ± 38, 111 ± 37, 81 ± 27		1128 ± 372, 564 ± 186	204 ± 67, 85 ± 28

https://doi.org/10.5194/egusphere-2023-1397
Preprint. Discussion started: 28 July 2023

Table 4. GZW Durations arranged by Ross Sea shelf position with uncertainty. OCS = outer continental shelf; MCS = middle continental shelf; IR = inner reaches.

4 Discussion

4.1 Stillstand Durations in Ross Sea

4.1.1 Millennial scale stillstand durations on the outer and middle continental shelf

The largest GZWs in the Ross Sea suggests that stillstands lasted up to a few millennia (Table 4). This general assessment is strongly supported by radiocarbon dates of the WDB middle continental shelf (MCS) stillstand (Bart et al., 2018). The Ross Sea GZWs are significantly larger than those on the outer reaches of other Antarctic margins (Batchelor and Dowdeswell, 2015). Their larger sediment volumes are partly related to ice stream erosion across the broad West Antarctic catchment areas, much of which is underlain by sedimentary rock (Tinto et al., 2019). The high sediment flux and widespread sediment aggradation at the grounding lines (Table 3) would have also contributed to long stillstands by countering the effect of ice-stream thinning associated with the deglaciation as flow accelerates, sea-level rises and global climates warm (Anandakrishnan et al., 2007).

4.1.2 Variable stillstand durations from trough to trough

Our data show that the Ross Sea stillstands were of millennial and centennial durations. Here, we focus on comparisons to WDB MCS stillstand because its duration is constrained by radiocarbon dates (Bart et al., 2018). In map view, the WDB MCS appears to be in regional alignment to the OCS GZWs in DT and JB, and the MCS GZWs in PT, GCB and LAB (Figure 4). Within the duration uncertainties, the MCS stillstands of the WDB, DT and JB all could have lasted three millennium (Table 5). In contrast, the MCS GZWs in the PT, GCB and LAB have shorter stillstand durations. For those shorter stillstands to have all been of the millennial duration, the erosion rates would have to been outside of the range presented in Bart and Tulacyzk (2020). Erosion in the GCB catchment would have had to have averaged 0.3 mm/yr for its MCS stillstand to have matched the duration of the WDB MCS stillstand. The erosion rates for the PT and LAB would have been even lower, averaging only 0.1

https://doi.org/10.5194/egusphere-2023-1397
Preprint. Discussion started: 28 July 2023

mm/yr. Such low erosion rates are not tenable with the deglacial timeframe during which ice flow and yields increase (Elverhøi et al., 1998; Davies et al., 2018).

Stratigraphic superpositions	Little America	Whales Deep	Glomar Challenger	Pennell	JOIDES	Drygalski
1. OCS	0.8	0.3	0.3			0.5
2. MCS	0.4	0.7	0.3	0.1	0.9	
3. Inner Reaches MCS	0.1		0.03, 0.02, 0.02		0.3, 0.1	0.05, 0.02

Table 5: Sediment yield (mm yr^{-1}) to make all durations 3200 years

4.1.3 Stillstand durations within individual troughs

By stratigraphic super-position, GZWs on the OCS are older than those on the MCS. Within those basins with more than one GZW, e.g., LAB, our data suggests significant reductions in stillstand durations as the deglacial progressed. The shift to shorter stillstands on the inner reaches of the MCS is generally consistent with tenets of the marine-ice-sheet-instability hypothesis which predict unstable grounding line retreat across the foredeepened continental shelf (Weertman, 1974). Grounding zone deposits that are too small or thin to map with seismic data are reported from several of the Ross Sea troughs from high-resolution swath bathymetry (Halberstadt et al., 2016; Simkins et al., 2017; Greenwood et al., 2018; Bart and Kratochvil, 2022). We follow other studies that suggest these small-scale features would logically correspond to decadal and/or annual timeframes (Livingstone et al., 2016; Dowdeswell et al., 2019).

4.2 On the post-LGM erosion rates in Ross Sea

A key assumption of our study is that erosion rates ranged from 0.7 ± 0.21 mm/yr. This relatively broad range overlaps with the erosion rate estimates for modern WAIS ice stream (Alley et al., 1986, 1987). The yields are also within the range of erosion for land-based glaciers from Norway, Svalbard and Switzerland and upper-slope Bear Island trough mouth fan depocenters (Elverhøi et al., 1998). These and other studies show that yield is affected by the degree of ice cover, regional climate, the associated precipitation, and presence/absence of meltwater. All the Ross Sea catchments are south of 70°S and over the post-LGM timeframes we considered, the climates were uniformly colder than present (Cuffey et al., 2016). The catchments were all 100% covered by grounded ice so the degree of glaciation could not have been a significant contributor to erosion rate differences between drainage areas. There is no evidence of warmer-than-present intervals that might have significantly increased meltwater production that would have contributed to high end erosion rates (Cuffey et al., 2016). Other important factors that influence yield include the areal extent of the catchment, the erodibility of substrate and the rate of ice flow (Hallet et al., 1996). The lowest erosion rates are expected for large catchments with slow-flowing cold ice (Elverhøi et al., 1998). Deglacial erosion rates are expected to be high because of the rapid flow of warmer ice (Kingslake et al., 2018; Koppes and Montgomery, 2009). The difference in the areas of Ross Sea catchments is relatively small and hence the post-LGM erosion rates are not expected to have significantly varied from trough to trough. All of West Antarctica is underlain by sedimentary strata save for small areas of exposed basement and hence substrates are expected to have similar erodibilities (Wilson and Luyendyk, 2006). The East Antarctica parts of the Ross Sea catchments are underlain by less erodible metamorphic and igneous rocks but yields from basement rock are lower by only 30% compared to sedimentary strata (Schlunegger and Hinderer, 2001). We dismiss the possibility that post-LGM erosion rates across East Antarctic catchments to Ross Sea were on average lower than the Bart and Tulacyzk (2020) low- end estimate of 0.7 ±0.21 mm/yr derived for WDB. The upper-end of the WDB erosion rate estimate is associated with rapid flow following an ice shelf breakup where ice-stream flow is estimated to have accelerated to 1350 m/yr from 200 m/yr (Tulaczyk and Bart, 2020). On these bases, we propose that our first-order estimates are appropriate for comparing grounding stillstand durations.

4.3 A staggered post-LGM retreat of WAIS grounding lines in Ross Sea

Grounding line retreat from the DT OCS stillstand is estimated to have occurred at 16.5 kyr BP (Prothro et al., 2020; Anderson et al., 2014). Prothro et al. (2020) used benthic foraminifera from glacial proximal sediments to show that middle shelf grounding zone stillstands in the JB and PT ended at 15.1 kyr BP and 13.3 kyr BP respectively. Radiocarbon dates from the WDB show that ice had retreated from the shelf edge by 14.7 ± 0.3 cal kyr BP and that retreat from the MCS occurred at 11.5 ± 0.3 cal kyr BP (Bart et al., 2018). Bart and Cone (2012) proposed the GCB stillstand ended at 27.5 cal kyr BP. A pre-LGM retreat is precluded because data presented by Halberstadt et al. (2016) require that ice remained grounded in both GCB and

https://doi.org/10.5194/egusphere-2023-1397
Preprint. Discussion started: 28 July 2023

LAB until after a grounding line embayment opened in the WDB at 11.5 cal kyr BP (Bart and Kratochvil, 2022). The oldest date from deglacial sediment overlying the foreset of the MCS GZW in GCB requires that the stillstand had ended by 8715 cal yr BP (Bart and Cone, 2012). We apply the same age of retreat (8715 cal yr BP) to the LAB MCS stillstand because the only other radiocarbon ages are from core tops.

Our data do not support previous studies that suggested that retreat occurred in a gradual lockstep fashion (Conway et al., 1999). Instead, both the chronology and stillstand duration data suggest that grounding line retreat proceeded in an unsteady fashion that was staggered from trough to trough (Table 6 and Figure 5). The earliest retreat in DT may be partly related to the greater depth of the DT. The subsequent opening of an embayment in PT may have been related to its small catchment area that delivered relatively-small volumes of ice to the grounding zone. The sustained grounding in the JB may have been associated with both its larger catchment, flow capture from the PT catchment and buttressing from its adjacent broad shallow banks. The long stillstand duration in the WDB may have been aided by antecedent topography that includes a bottleneck constriction at the location of the MCS grounding stillstand (Danielson and Bart, 2019) plus the apparent rapid sediment aggradation following ice shelf break up at 12.3 cal kyr BP (Bart and Tulaczyk, 2020). The available age control (see above) suggests that up to three millennia may have elapsed before grounded ice retreated from the GCB and LABs but here the chronologies are poorly constrained.

We acknowledge that the retreat chronology is likely to change as more radiocarbon data are generated. With the available constraints, our data supports other previous studies that suggested that retreat was not synchronous or in lock step from trough to trough (Halberstadt et al., 2016; Prothro et al., 2020; Mosola and Anderson, 2006). Neither the onset, duration or termination of Ross Sea stillstands appear to be related to global or regional scale forcing mechanism with the possible exception of the WDB MCS stillstand which may be bracketed between intervals of rapid, large amplitude sea-level rise at MWPs 1a and 1b (Lin et al., 2021). These data are not consistent with the view that WAIS contraction in Ross Sea contributed significantly to the sustained sea-level rise during either MWP1a or 1b. An asynchronous opening of grounding-line embayments would have been associated with multiple episodes of short-lived accelerated sea-level rise. The marked sinuosity of the current grounding line in Ross Sea suggests that this style of staggered retreat style persists through to present.

https://doi.org/10.5194/egusphere-2023-1397
Preprint. Discussion started: 28 July 2023

GZW Wedge Location	Retreat mode Duration, ΔT (yr)	Nearest retreat date (cal yr BP)	Grounding start date (cal yr BP)	Date Reference
b. LAB Middle Shelf	1535	$8715_b \pm 70$	10250 ± 70	NBP0802 PC2 7 - 9 cm (Bart and Cone, 2012)
e. WDB Middle Shelf	3200	$11500_b \pm 300$	14701 ± 300	NBP1502B KC07 (Bart et al., 2018)
g. GCB Middle Shelf West	1379	$8715_b \pm 50$	9926 ± 50	NBP0802 PC2 7 - 9 cm (Bart and Cone, 2012)
k. PT Middle Shelf	604	$15121_b \pm 270$	15725 ± 270	NBP1502A KC17 144 – 145 cm (Prothro et al., 2020)
l. JOIDES Middle Shelf	3433	$13315_a \pm 240$	16748 ± 240	NBP1502A KC48 Prothro et al., 2020;
o. DT Outer Shelf	2280	16519b ± 260	18799 ± 260	NBP9501 KC37 (Prothro et al., 2020; Anderson 2014)

a: AIO bulk sediment date

b: Benthic carbonate material from grounding zone sedimentation

Table 6: Grounding start date model for MCS GZWs

https://doi.org/10.5194/egusphere-2023-1397
Preprint. Discussion started: 28 July 2023

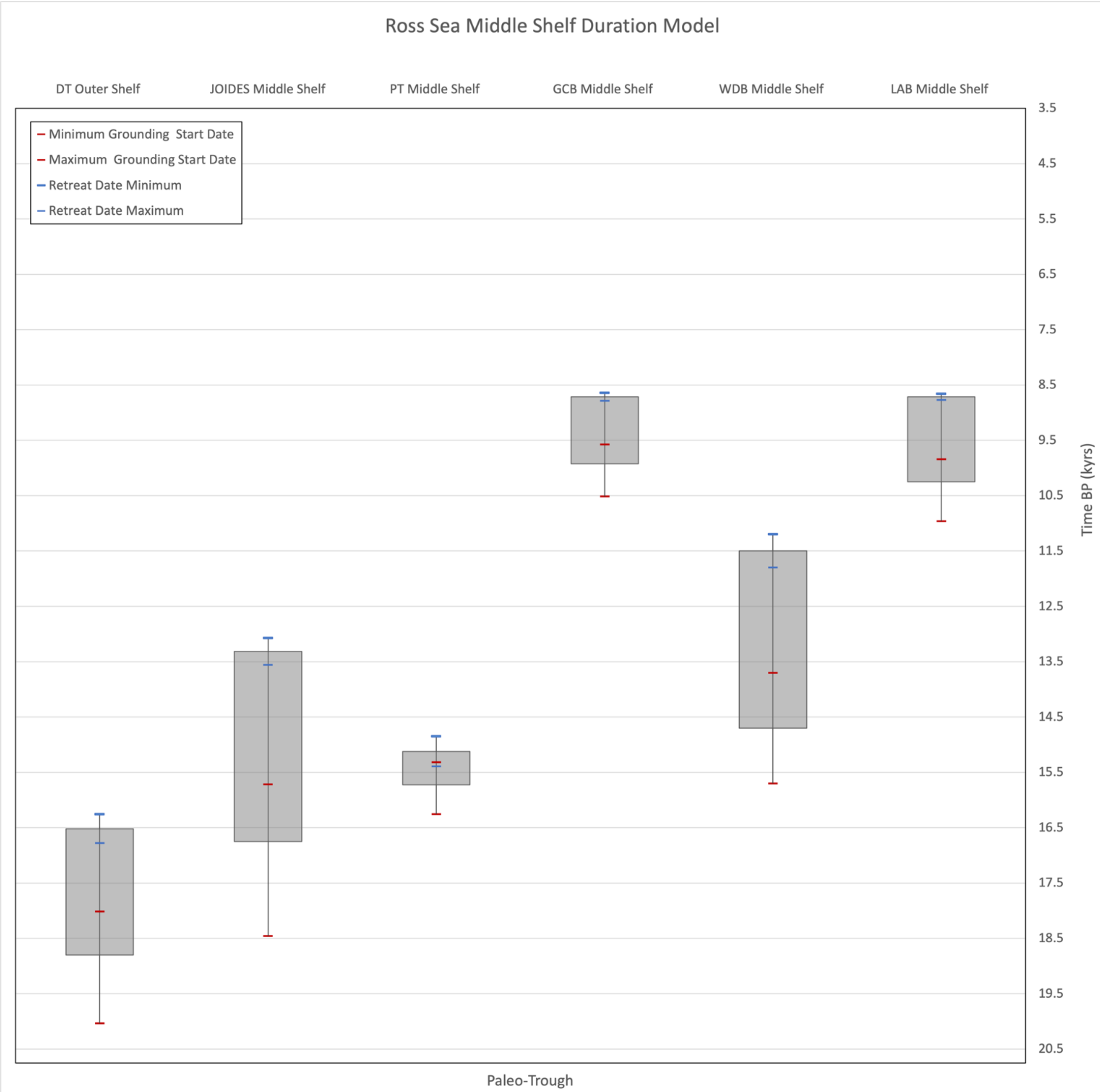

Figure 5. Duration age model for the MCS GZWs in Ross Sea using the durations and nearest retreat date plotted in Table 6. The grey box shows the median grounding zone retreat date added to the estimated duration to yield a grounding start date. Blue markers show the uncertainty of the retreat date. Red markers show the uncertainty of the retreat date added to the duration yielding

https://doi.org/10.5194/egusphere-2023-1397
Preprint. Discussion started: 28 July 2023

minimum and maximum grounding start dates. The uncertainty of the duration estimates is incorporated in the minimum and maximum start dates.

5 Conclusion

The locations and sediment volumes of GZWs suggest millennial to centennial duration stillstands for Ross Sea ice streams during the early phases of the post-LGM retreat. Combined with the available age control, our first-order duration estimates require a staggered retreat from trough to trough that formed deep grounding-line embayments. Asynchronous collapse of individual catchments occurring over the course of the post-LGM suggests that the Ross Sea sector would have contributed to multiple episodes of small amplitude, sea-level rise. The high sinuosity of the modern ground zone in Ross Sea suggests that this retreat style persists.

Data Availability

The data that support the findings of this study are openly available in the SDLS hosted at OGS at https://sdls.ogs.trieste.it/cache/index.jsp. A full list of seismic surveys used in this study are listed in Supplemental Table 1.

Author contribution

MD performed the mapping of the seismic data and figure generation; MD and PB interpreted the results.; MD and PB wrote and edited the manuscript.

Competing interests

The authors declare that they have no conflict of interest.

Acknowledgments

Support for the project was provided by a United States National Science Foundation Office of Polar Programs Antarctic Earth Sciences Division grant (#1841136) to Bart. Seismic data used for this project were accessed from the Antarctic Seismic Data

Library System (SDLS) hosted at the National Institute of Oceanography and Applied Geophysics (OGS). We thank the original collectors of these data. A full list of the seismic surveys used can be found in supplemental table 1.

References

Alley, R. B., Blankenship, D. D., Bentley, C. R., and Rooney, S. T.: Deformation of till beneath ice stream B, West Antarctica, Letters to Nature, 322, 57-59, 1986.

Alley, R. B., Blankenship, D. D., Bentley, C. R., and Rooney, S. T.: Till beneath ice stream B: 3. Till deformation: Evidence and implications, Journal of Geophysical Research, 92, 10.1029/JB092iB09p08921, 1987.

Alley, R. B., Blankenship, D. D., Rooney, S. T., and Bentley, C. R.: Sedimentation beneath ice shelves - the view from ice stream B., Marine Geology, 85, 101-120, 1989.

Alley, R. B., Anandakrishnan, S., Dupont, T. K., Parizek, B. R., and Pollard, D.: Effect of Sedimentation on Ice-Sheet Grounding-Line Stability, Science Reports, 315, 1838 - 1840, 2007.

Anandakrishnan, S., Catania, G. A., Alley, R. B., and Horgan, H. J.: Discovery of Till Deposition at the Grounding Line of Whillans Ice Stream, Science Reports, 315, 1835 - 1837, 2007.

Anderson, J. B., Conway, H., Bart, P. J., Witus, A. E., Greenwood, S. L., McKay, R. M., Hall, B. L., Ackert, R. P., Licht, K., Jakobsson, M., and Stone, J. O.: Ross Sea paleo-ice sheet drainage and deglacial history during and since the LGM, Quaternary Science Reviews, 100, 31-54, 10.1016/j.quascirev.2013.08.020, 2014.

Baroni, C., Tenti, M., Bart, P., Salvatore, M. C., Gasperini, L., Busetti, M., Sauli, C., Stucchi, E. M., and Tognarelli, A.: Antarctic Ice Sheet re-advance during the Antarctic Cold Reversal identified in the Western Ross Sea, GEOGRAFIA FISICA E DINAMICA QUATERNARIA, 45, 3-18, 2022.

Bart, P. and De Santis, L.: Glacial Intensification During the Neogene: A Review of Seismic Stratigraphic Evidence from the Ross Sea, Antarctica, Continental Shelf, Oceanography, 25, 166-183, 10.5670/oceanog.2012.92, 2012.

Bart, P. J. and Cone, A. N.: Early stall of West Antarctic Ice Sheet advance on the eastern Ross Sea middle shelf followed by retreat at 27,50014CyrBP, Palaeogeography, Palaeoclimatology, Palaeoecology, 335-336, 52-60, 10.1016/j.palaeo.2011.08.007, 2012.

Bart, P. J. and Kratochvil, M.: A paleo-perspective on West Antarctic Ice Sheet retreat, Sci Rep, 12, 17693, 10.1038/s41598-022-22450-3, 2022.

Bart, P. J. and Owolana, B.: On the duration of West Antarctic Ice Sheet grounding events in Ross Sea during the Quaternary, Quaternary Science Reviews, 47, 101-115, 10.1016/j.quascirev.2012.04.023, 2012.

Bart, P. J. and Tulaczyk, S.: A significant acceleration of ice volume discharge preceded a major retreat of a West Antarctic paleo–ice stream, Geology, 48, 313-317, 10.1130/g46916.1, 2020.

Bart, P. J., Krogmeier, B. J., Bart, M. P., and Tulaczyk, S.: The paradox of a long grounding during West Antarctic Ice Sheet retreat in Ross Sea, Sci Rep, 7, 1262, 10.1038/s41598-017-01329-8, 2017.

Bart, P. J., DeCesare, M., Rosenheim, B. E., Majewski, W., and McGlannan, A.: A centuries-long delay between a paleo-ice-shelf collapse and grounding-line retreat in the Whales Deep Basin, eastern Ross Sea, Antarctica, Sci Rep, 8, 12392, 10.1038/s41598-018-29911-8, 2018.

Batchelor, C. L. and Dowdeswell, J. A.: Ice-sheet grounding-zone wedges (GZWs) on high-latitude continental margins, Marine Geology, 363, 65-92, 10.1016/j.margeo.2015.02.001, 2015.

Christoffersen, P., Tulaczyk, S., and Behar, A.: Basal ice sequences in Antarctic ice stream: Exposure of past hydrologic conditions and a principal mode of sediment transfer, Journal of Geophysical Research, 115, 10.1029/2009jf001430, 2010.

Cochrane, G. R., De Santis, L., and Cooper, A. K.: Seismic velocity expression of glacial sedimentary rocks beneath the Ross Sea from sonobuoy seismic-refraction data, Geology and Seismic Stratigraphy of the Antarctic Margin: Antarctic Research Series, 68, 261 - 270, 1995.

Cochrane, G. R., Cooper, A. K., Childs, J. R., and Hart, P. E.: USGS seismic refraction surveys in the Ross Sea, 1984-1990, USGS Openfile Reports, 92-556, 1992.

Conway, H., Hall, B. L., Denton, G. H., Gades, A. M., and Waddington, E. D.: Past and Future Grounding-Line Retreat of the West Antarctic Ice Sheet, Science, 286, 280-283, 10.1126/science.286.5438.280, 1999.

Cuffey, K. M., Clow, G. D., Steig, E. J., Buizert, C., Fudge, T. J., Koutnik, M., Waddington, E. D., Alley, R. B., and Severinghaus, J. P.: Deglacial temperature history of West Antarctica, Proc Natl Acad Sci U S A, 113, 14249-14254, 10.1073/pnas.1609132113, 2016.

Davies, D., Bingham, R. G., King, E., Smith, A. M., Brisbourne, A. M., Spagnolo, M., Graham, A. G. C., Hogg, A. E., and Vaughan, D. G.: How dynamic are ice-stream beds?, The Cryosphere, 12, 1615 - 1528, 2018.

Domack, E. W., Jacobson, E. A., Shipp, S., and Anderson, J. B.: Late Pleistocene–Holocene retreat of the West Antarctic Ice-Sheet system in the Ross Sea: Part 2—Sedimentologic and stratigraphic signature, Geological Society of America Bulletin, 111, 1517–1536, 1999.

Dowdeswell, J. A., Hogan, K. A., and Le Heron, D. P.: The glacier-influenced marine record on high-latitude continental margins: synergies between modern, Quaternary and ancient evidence, Geological Society, London, Special Publications, 475, 261-279, 10.1144/sp475.13, 2019.

Elverhøi, A., Hooke, R. L., and Solheim, A.: LATE CENOZOIC EROSION AND SEDIMENT YIELD FROM THE SVALBARDÐBARENTS SEA REGION: IMPLICATIONS FOR UNDERSTANDING EROSION OF GLACIERIZED BASINS, Quaternary Science Reviews, 17, 209 - 241, 1998.

Greenwood, S. L., Simkins, L. M., Halberstadt, A. R. W., Prothro, L. O., and Anderson, J. B.: Holocene reconfiguration and readvance of the East Antarctic Ice Sheet, Nat Commun, 9, 3176, 10.1038/s41467-018-05625-3, 2018.

Halberstadt, A. R. W., Simkins, L. M., Greenwood, S. L., and Anderson, J. B.: Past ice-sheet behaviour: retreat scenarios and changing controls in the Ross Sea, Antarctica, The Cryosphere, 10, 1003-1020, 10.5194/tc-10-1003-2016, 2016.

https://doi.org/10.5194/egusphere-2023-1397
Preprint. Discussion started: 28 July 2023

Hallet, B., Hunter, L., and Bogen, J.: Rates of erosion and sediment evacuation by glaciers: A review of field data and their implications Global and Planetary Change, 12, 213 -235, 1996.

Kingslake, J., Scherer, R. P., Albrecht, T., Coenen, J., Powell, R. D., Reese, R., Stansell, N. D., Tulaczyk, S., Wearing, M. G., and Whitehouse, P. L.: Extensive retreat and re-advance of the West Antarctic Ice Sheet during the Holocene, Nature, 558, 430-434, 10.1038/s41586-018-0208-x, 2018.

Koppes, M. N. and Montgomery, D. R.: The relative efficacy of fluvial and glacial erosion over modern to orogenic timescales, Nature Geoscience, 2, 644-647, 10.1038/ngeo616, 2009.

Licht, K. J. and Palmer, E. F.: Erosion and transport by Byrd Glacier, Antarctica during the Last Glacial Maximum, Quaternary Science Reviews, 62, 32-48, 10.1016/j.quascirev.2012.11.017, 2013.

Licht, K. J., Hennessy, A. J., and Welke, B. M.: The U-Pb detrital zircon signature of West Antarctic ice stream tills in the Ross embayment, with implications for Last Glacial Maximum ice flow reconstructions, Antarctic Science, 26, 687-697, 10.1017/s0954102014000315, 2014.

Licht, K. J., Lederer, J. R., and Jeffrey Swope, R.: Provenance of LGM glacial till (sand fraction) across the Ross embayment, Antarctica, Quaternary Science Reviews, 24, 1499-1520, 10.1016/j.quascirev.2004.10.017, 2005.

Lin, Y., Hibbert, F. D., Whitehouse, P. L., Woodroffe, S. A., Purcell, A., Shennan, I., and Bradley, S. L.: A reconciled solution of Meltwater Pulse 1A sources using sea-level fingerprinting, Nat Commun, 12, 2015, 10.1038/s41467-021-21990-y, 2021.

Livingstone, S. J., Stokes, C. R., Ó Cofaigh, C., Hillenbrand, C.-D., Vieli, A., Jamieson, S. S. R., Spagnolo, M., and Dowdeswell, J. A.: Subglacial processes on an Antarctic ice stream bed. 1: Sediment transport and bedform genesis inferred from marine geophysical data, Journal of Glaciology, 62, 270-284, 10.1017/jog.2016.18, 2016.

Mosola, A. B. and Anderson, J. B.: Expansion and rapid retreat of the West Antarctic Ice Sheet in eastern Ross Sea: possible consequence of over-extended ice streams?, Quaternary Science Reviews, 25, 2177-2196, 10.1016/j.quascirev.2005.12.013, 2006.

Powell, R. D., Dawber, M., McInnes, J. N., and Pyne, A. R.: Observations of the grounding-line area at a floating glacier terminus, Annals of Glaciology, 22, 217-223, 10.3189/1996AoG22-1-217-223, 1996.

Prothro, L. O., Simkins, L. M., Majewski, W., and Anderson, J. B.: Glacial retreat patterns and processes determined from integrated sedimentology and geomorphology records, Marine Geology, 395, 104-119, 10.1016/j.margeo.2017.09.012, 2018.

Prothro, L. O., Majewski, W., Yokoyama, Y., Simkins, L. M., Anderson, J. B., Yamane, M., Miyairi, Y., and Ohkouchi, N.: Timing and pathways of East Antarctic Ice Sheet retreat, Quaternary Science Reviews, 230, 10.1016/j.quascirev.2020.106166, 2020.

Schlunegger, F. and Hinderer, M.: Crustal uplift in the Alps: why the drainage pattern matters, Terra Nova, 13, 425 - 432, 2001.

Shipp, S., Anderson, J., and Domack, E.: Late Pleistocene–Holocene retreat of the West Antarctic Ice-Sheet system in the Ross Sea: Part 1—Geophysical results, Geological Society of America Bulletin, 111, 10.1130/0016-7606(1999)111<1486:Lphrot>2.3.Co;2, 1999.

https://doi.org/10.5194/egusphere-2023-1397
Preprint. Discussion started: 28 July 2023

Simkins, L. M., Anderson, J. B., Greenwood, S. L., Gonnermann, H. M., Prothro, L. O., Halberstadt, A. R. W., Stearns, L. A., Pollard, D., and DeConto, R. M.: Anatomy of a meltwater drainage system beneath the ancestral East Antarctic ice sheet, Nature Geoscience, 10, 691-697, 10.1038/ngeo3012, 2017.

Tinto, K. J., Padman, L., Siddoway, C. S., Springer, S. R., Fricker, H. A., Das, I., Caratori Tontini, F., Porter, D. F., Frearson, N. P., Howard, S. L., Siegfried, M. R., Mosbeux, C., Becker, M. K., Bertinato, C., Boghosian, A., Brady, N., Burton, B. L., Chu, W., Cordero, S. I., Dhakal, T., Dong, L., Gustafson, C. D., Keeshin, S., Locke, C., Lockett, A., O'Brien, G., Spergel, J. J., Starke, S. E., Tankersley, M., Wearing, M. G., and Bell, R. E.: Ross Ice Shelf response to climate driven by the tectonic imprint on seafloor bathymetry, Nature Geoscience, 12, 441-449, 10.1038/s41561-019-0370-2, 2019.

Tulaczyk, S. and Bart, P. J.: A significant acceleration of ice volume discharge preceded a major retreat of a West Antarctic paleo–ice stream, Geology, 48, 313-317, 10.1130/g46916.1, 2020.

Weertman, J.: Stability of the Junction of an Ice Sheet and an Ice Shelf, Journal of Glaciology, 13, 3-11, 10.3189/s0022143000023327, 1974.

Wilson, D. S. and Luyendyk, B. P.: Bedrock platforms within the Ross Embayment, West Antarctica: Hypotheses for ice sheet history, wave erosion, Cenozoic extension, and thermal subsidence, Geochemistry, Geophysics, Geosystems, 7, n/a-n/a, 10.1029/2006gc001294, 2006.